Cellular/Molecular

Synaptic Acidification Enhances $GABA_A$ Signaling

Craig J. Dietrich[1] **and Martin Morad**[1,2]

[1]Interdisciplinary Program in Neuroscience and Department of Pharmacology, Georgetown University School of Medicine, Washington, DC 20007, and [2]Cardiac Signaling Center, University of South Carolina, Medical University of South Carolina, and Clemson University, Charleston, South Carolina 29425

To determine the role of cellularly generated protons in synaptic signaling, we recorded GABA miniature IPSCs (mIPSCs) from cultured rat cerebellar granule cells (CGCs) while varying the extracellular pH buffering capacity. Consistent with previous reports, we found that increasing pH from 7.4 to 8.0 sped mIPSC rise time and suppressed both amplitude of the current and total charge transferred. Conversely, acidification (from pH 7.4 to 6.8) slowed the rise time and increased current amplitude and total charge transferred. In a manner consistent with alkalinization, increasing the buffering capacity from 3 to 24 mM HEPES at pH 7.4 resulted in faster mIPSC rise time, a 37% reduction in amplitude, and a 48% reduction in charge transferred. Supplementing the normal physiological buffers (24 mM HCO_3^-/5%CO_2) with 10 mM HEPES similarly diminished mIPSCs in a manner consistent with alkalinization, resulting in faster rise time, a 39% reduction in amplitude, and a 51% reduction in charge transferred. These findings suggest the existence of an acidifying synaptic force that is overcome by commonly used concentrations (10 mM) of HEPES buffer. Here we show that Na^+/H^+ exchanger (NHE) activity appears to, in part, contribute to this synaptic acidification because inhibition of NHE by amiloride or lithium under physiological or weak buffering conditions alters mIPSCs in a manner consistent with alkalinization. These results suggest that acidification of the synaptic cleft occurs physiologically during GABAergic transmission and that NHE plays a critical role in generating the acidic nano-environment at the synapse.

Introduction

In the brain, pH is critically linked to proper neuronal function (Kaila and Ransom, 1998). The discovery of proton-gated acid-sensing ion channels (ASICs) (Krishtal and Pidoplichko, 1981; Waldmann and Lazdunski, 1998), coupled with the acute pH sensitivities of voltage-gated calcium channels (VGCCs) (Iijima et al., 1986) and ligand-gated NMDA receptors (NMDARs) (Tang et al., 1990; Traynelis and Cull-Candy, 1990) and GABA receptors (GABARs) (Kaila, 1994), suggests that pH regulation plays a crucial role in synaptic signaling. Considerable effort has been made to identify and quantify extracellular neuronal pH shifts (Kraig et al., 1983; Chesler and Kaila, 1992). Although high-speed pH electrodes (Fedirko et al., 2006) and dyes (Shuba et al., 2008) provide reliable assessment of pH changes in the extracellular space, they cannot probe the functionally critical nano-domains of the synapse.

Although evidence for endogenous synaptic pH fluctuations is scarce, it is known that (1) presynaptic VGCCs at retinal ribbon synapses are inhibited by vesicular proton release (DeVries, 2001; Palmer et al., 2003), (2) hippocampal NMDA currents are potentiated by a transient loss of protons (Makani and Chesler, 2007), and (3) ASIC-like channels in *Caenorhabditis elegans* muscle wall are activated by proton release from an Na^+/H^+ exchanger (NHE) homolog (Beg et al., 2008).

Here we attempt to clarify the role of protons in mammalian central inhibitory neurotransmission by assessing the endogenous pH modulation of the synapse and its subsequent postsynaptic impact. To this end, we have chosen to study GABAergic miniature IPSCs (mIPSCs) in cultured rat cerebellar granule cells (CGCs). As opposed to proton-inhibited NMDARs, GABAR response is enhanced by acidification (Kaila, 1994), and thus confounds of interpretation caused by proton inhibition of presynaptic VGCCs (Iijima et al., 1986) are alleviated. Furthermore, the effects of pH on $GABA_A$ receptors in rat CGCs (Robello et al., 1994) and on mIPSC size and kinetics are well characterized (Mozrzymas et al., 2003). Our experimental manipulation was simple: we modulated the proton buffering capacity of the synapse by varying the HEPES concentration of superfusing solutions. This method has been validated in studies of endogenous proton modulation of presynaptic VGCCs (DeVries, 2001; Palmer et al., 2003) and allows rapid, reliable washout to test reversibility.

We report for the first time that mIPSCs recorded at pH 7.4 under conditions of either physiological bicarbonate buffering or physiologically equivalent HEPES buffering (Palmer et al., 2003) ("unclamped pH_o") are nearly identical in size and kinetics to those recorded at pH 6.8 under conditions of strong HEPES buffering ("clamped pH_o"). Furthermore, "clamping" pH_o at 7.4 caused changes to mIPSCs amplitude and kinetics consistent with alkalinization (Mozrzymas et al., 2003) when compared with "unclamped" control events. These results suggest an acidifying force is present at the GABAergic synapse. We show that selective inhibition of the NHE with either amiloride or lithium alters mIPSCs in a manner identical to either increasing proton buffering capacity or alkalinization. We propose that endogenous proton buffering at the GABAergic synapse is sufficiently weak as to allow its acidification and posit that proton extrusion via the NHE plays a critical role in shaping the pH of these synaptic nano-domains.

Received Dec. 18, 2009; revised July 22, 2010; accepted July 26, 2010.

This work was funded by National Institutes of Health Grants R01HL016152 and T32NS041218.

Correspondence should be addressed to Martin Morad, Medical University of South Carolina, 173 Ashley Avenue, Room BSB319B, P.O. Box 25058, Charleston, SC 29425. E-mail: moradm@musc.edu.

DOI:10.1523/JNEUROSCI.6364-09.2010

Copyright © 2010 the authors 0270-6474/10/3016044-09$15.00/0

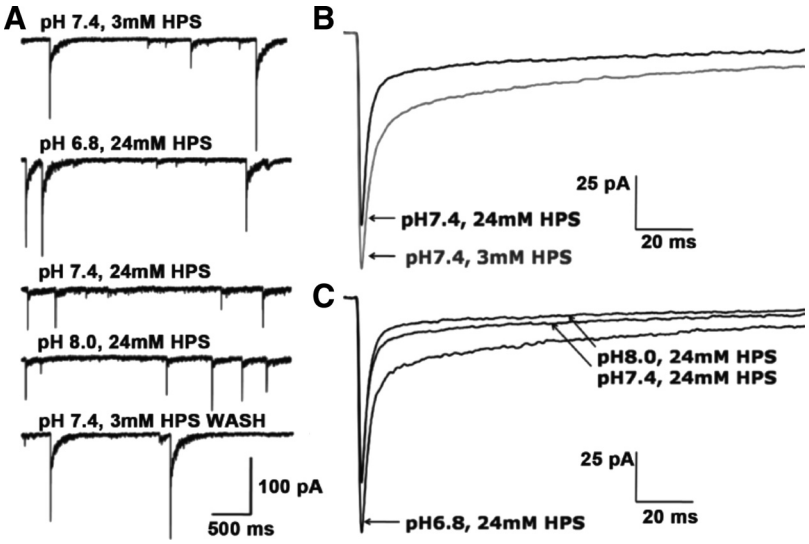

Figure 1. mIPSCs are enhanced by extracellular protons and diminished by increased buffer capacity. ***A***, Raw trace from one CGC at holding potential −60 mV illustrates GABA mIPSC response to changes in extracellular pH and buffering capacity. ***B***, Averaged traces ($n > 100$ events per condition) from one CGC under constant pH shows the effect of increased buffer capacity on mIPSCs. ***C***, Averaged traces ($n > 100$ events per condition) from one CGC under constant buffer capacity shows the effects of pH on mIPSCs. HPS, HEPES (in all figures).

Materials and Methods

Cell culture. Cerebellar cortices were dissected from postnatal day 7 Sprague Dawley rat pups. Pups were both male and female. Neurons were dissociated mechanically and then enzymatically in 0.25 mg/ml trypsin (Sigma) and plated at a density of 1.1×10^6 cells/ml on glass coverslips coated with poly-D-lysine at 10 μg/ml (Sigma) in 35 mm Nunc dishes in basal medium Eagle's supplemented with 10% FBS, 2 mM glutamine, and 100 μg/ml gentamycin (all from Invitrogen), and KCl concentration was adjusted to 25 mM and maintained at 37°C in 5% CO_2. At day *in vitro* 5 (DIV 5), medium was replaced with low (5 mM) potassium MEM supplemented with 5 mg/ml glucose, 0.1 mg/ml transferrin, 0.035 mg/ml insulin, 2 mM glutamine, 20 μg/ml gentamycin (all from Invitrogen), and 10 μM cytosine arabinofuranoside (Sigma) as described previously (Chen et al., 2000).

Electrophysiology. Coverslips with CGCs were placed on the stage of an inverted microscope (Carl Zeiss) with phase-contrast optics. All recordings were performed at room temperature (24–26°C) from DIV 7–14 neurons. The recording chamber was continuously perfused at 5 ml/min with an extracellular solution (ECS) composed of the following (in mM): 145 NaCl, 5 KCl, 1 $MgCl_2$, 1 $CaCl_2$, 5 glucose, and either 3 HEPES with 27 sucrose, 10 HEPES with 20 sucrose, or 24 HEPES with 6 sucrose. pH was adjusted to 7.4 with NaOH. Bicarbonate-based solutions were composed of the following (in mM): 121 NaCl, 24 $NaHCO_3$, 5 KCl, 5 glucose, 30 sucrose, 1 $MgCl_2$, and 1 $CaCl_2$. For bicarbonate solutions supplemented with HEPES, the ECS was diluted by 3% and split into two parts, 5 mM NaCl was placed back into the "bicarbonate-only" portion to restore osmolarity, and 10 mEq HEPES was placed into the "HEPES" portion. All bicarbonate-containing solutions were bubbled under 5% CO_2/95% O_2. All solutions were verified iso-osmotic (~330 mOsm), and solution pH was verified before, during, and after experiments. For all recordings, KCl-based internal pipette solutions were used (in mM): 145 KCl, 10 HEPES, 10 tetraethylammonium-Cl, 1 EGTA, 5 ATP-Mg, and 0.02 GTP adjusted to pH 7.2 with KOH. In bicarbonate experiments, 24 mM $KHCO_3$ replaced a similar portion of KCl in the internal solution. Pipette resistance was 6–9 MΩ. Whole-cell voltage-clamp recordings were made at −60 mV with a Dagan 3900A amplifier, and access resistance was monitored throughout the recordings. Capacitance was calculated from a transient current response to a hyperpolarizing 10 mV pulse. Currents were filtered at 1 kHz with a four-pole low-pass Bessel filter and digitized at 5–20 kHz using an IBM-compatible computer equipped with Digidata 1322A data acquisition board and pClamp 9 software (both from Molecular Devices). mIPSCs were isolated by 0.5 μM TTX and 5 μM NBQX. NBQX was dissolved in DMSO; TTX, GABA, amiloride, and LiCl (all from Sigma) were dissolved in water and diluted in ECS. Drugs/test solutions were locally applied by means of rapid solution exchange (Davies et al., 1988), allowing total exchange in <200 ms in experiments in which exchange speed was not critical. mIPSC averages were made from 60–300 events in each cell studied. When GABA was applied exogenously, gravity flow force was increased such that exchange was sped to <50 ms. Cells were allowed to recover for 1 min between applications, and the measured values were recorded only after a consistent response was achieved over three consecutive applications. The average response to three GABA applications was used to obtain the values reported. Charge transfer values from GABA applications were standardized to a defined time point (generally 4 s) after onset of the current.

Analysis. Offline data analysis and curve fitting were performed with Clampfit 9.2 software. The decay phase of averaged currents were fitted using a Levenberg–Marquardt algorithm with a double-exponential equation of the form $I(t) = I1 * \exp(-t/\tau1) + I2 * \exp(-t/\tau2)$, where Ix is the peak current amplitude of a decay component, and τx is the corresponding decay time constant. To allow for easier comparison of decay times for flurazepam and exogenous GABA application experiments, the two decay time components were combined into a weighted time constant $\tau_w = [I1/(I1 + I2)] * \tau1 + [I2/(I1 + I2)] * \tau2$. The region searched for decay fits was from event peak to the end of the averaged trace (~300 ms after peak). All data are expressed as means ± SEM, unless otherwise noted. mIPSC values in experimental conditions were compared with events within the same cell at pH 7.4 in 3 mM HEPES (for HEPES-only experiments) or to 24 mM HCO_3^- (in bicarbonate buffer experiments). Student's *t* tests were used to determine significance. For comparisons across multiple groups, we used one-way ANOVAs followed by *post hoc* Bonferroni's multiple comparison *t* tests. Kolmogorov–Smirnov (K–S) tests were used to determine significance in cumulative probability histograms, whereas a Mann–Whitney *U* test was used for combined cumulative probability histograms.

Results

Increasing extracellular proton buffering capacity alters mIPSCs in a manner consistent with alkalinization

mIPSCs were recorded in the whole-cell configuration at a holding potential of −60 mV (Fig. 1*A*). Consistent with previous work (Mozrzymas et al., 2003) and now extended to cerebellar neurons, we found that extracellular pH below 7.4 enhanced GABAergic mIPSCs, whereas pH above 7.4 had the opposite effect (Fig. 1*C*). To probe the endogenous pH buffering capacity at the synapse, we compared the effects of strong proton buffering (10–24 mM HEPES) with weaker buffering (3 mM HEPES) reported to approximate physiological buffering (Palmer et al., 2003). We have defined mIPSC values recorded in 3 mM HEPES at pH 7.4 as quasi-physiological, controls. Frequency of events in 3 mM HEPES varied from cell to cell (0.87 ± 0.15 Hz; $n = 6$) but did not change significantly with increased buffering capacity ($p = 0.65$, ANOVA; $n = 6$), although there was a trend toward decreased frequency with acidification and increased frequency with alkalinization (supplemental Fig. S1*A*, available at www.jneurosci.org as supplemental material).

Because cell-to-cell amplitudes were highly variable (55.07 ± 5.67 pA), a combined cumulative probability distribution (Mathews and Diamond, 2003) was constructed to best deter-

mine significant differences between populations. Analysis reveals a significant shift in mIPSC amplitude attributable to increased buffering conditions ($p < 0.0001$, Mann–Whitney U test; $n = 1928$ events in control, 1748 events in 24 mM HEPES) (Fig. 2*A*). For comparisons across buffering and pH conditions, amplitudes were quantified relative to measurements in 3 mM HEPES. Increasing the buffering capacity at pH 7.4 and 8.0, respectively, reduced mIPSC amplitudes by ~35% ($p < 0.0001$; $n = 19$) and ~38% ($p < 0.05$; $n = 6$) with respect to control. Strong buffering at pH 6.8 did not differ from control ($p = 0.79$, ANOVA; $n = 6$) (supplemental Fig. S1*B*, available at www.jneurosci.org as supplemental material).

Consistent with previous reports that acidification slows mIPSC rise times (Mozrzymas et al., 2003), we found slower rise times in 3 mM HEPES than in strong buffering at pH 7.4 (supplemental Fig. S1*C*, available at www.jneurosci.org as supplemental material). A combined cumulative probability histogram from all neurons shows significant speeding (left shift) of rise time attributable to increased buffering ($p < 0.0001$, Mann–Whitney U test; $n = 1928$ events in control, 1748 events in 24 mM HEPES) (Fig. 2*B*). All mean rise times became faster with increased buffering at pH 7.4, and mean population rise time significantly sped from 0.638 ± 0.014 to 0.59 ± 0.014 ms ($p < 0.0001$, t test; $n = 19$) (supplemental Fig. S1*D*, available at www.jneurosci.org as supplemental material). Increased buffering capacity significantly sped rise time at pH 8.0 ($p < 0.05$, ANOVA; $n = 6$) but not at pH 6.8 (supplemental Fig. S1*E*, available at www.jneurosci.org as supplemental material) compared with quasi-physiological conditions.

Extracellular alkalinization speeds the fast component of mIPSC decay kinetics (τ_{fast}) but decreases the slow component (τ_{slow}) and increases the percentage contribution of the fast component to total decay (Mozrzymas et al., 2003). Our detailed analysis reveals that increased buffering has the same effect as alkalinization on decay kinetics (supplemental Fig. S2, available at www.jneurosci.org as supplemental material).

Together, mIPSC amplitude and decay kinetics describe the total charge transferred by the synaptic event. Figure 2*C* graphs the charge transfer in all neurons under both buffering conditions at pH 7.4. The average charge transfer measured in control plotted against strong buffering in the same neuron yields the scatter plot. All points lie below unity (solid dark line), indicating consistently greater charge transfer in 3 versus 24 mM HEPES buffering. The gray dashed line represents regression through all points; the high R^2 value (0.8667) indicates the strong consistency of effect. The gray point denotes the population means charge transfer (1.86 ± 0.21 pC in 3 mM HEPES vs 0.94 ± 0.1 pC in 24 mM HEPES). Strong buffering at pH 7.4 decreased charge transfer by ~48% compared with control ($p < 0.0001$, ANOVA; $n = 19$) and by ~64.1% at pH 8.0 ($p < 0.0001$, ANOVA; $n = 6$) but had little effect at pH 6.8 on total charge transfer relative to control. As additional evidence of proton effect, changing from pH 6.8 to 7.4 in strong buffer conditions (24 mM HEPES) decreased charge transfer by 44%, ($p < 0.01$, t test; $n = 6$), and the decrease was 18% from pH 7.4 to 8.0 ($p < 0.01$, ANOVA; $n = 6$) (Fig. 2*D*). These results indicate that increasing the buffering capacity of the extracellular solution is equivalent to alkalinizing the GABAergic synapse. Together, the data suggest that synaptic cleft pH is not clamped at pH 7.4, as is generally assumed, but may change significantly during synaptic activity.

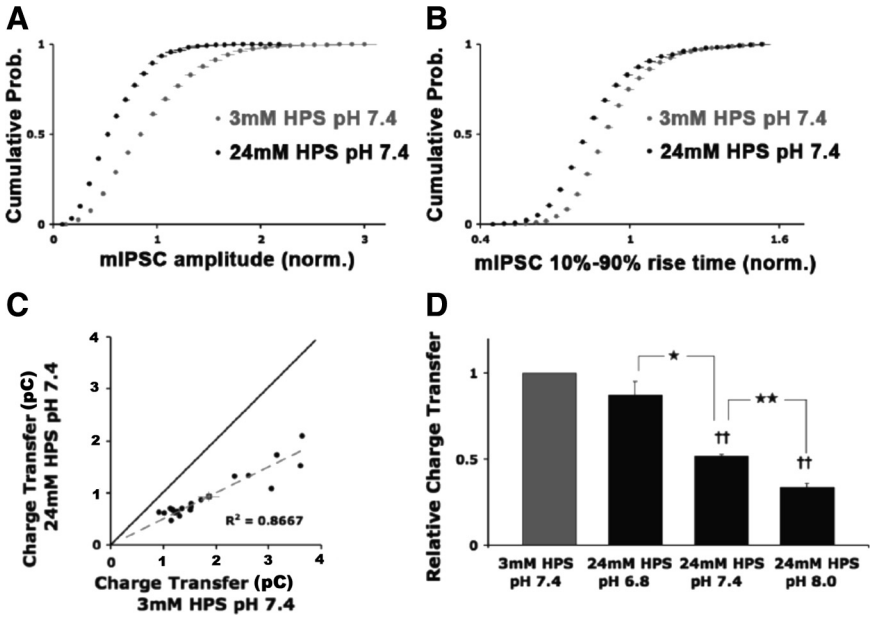

Figure 2. Extracellular protons and proton buffering modulate amplitude, rise time, and charge transfer of GABAergic mIPSCs in CGCs. ***A***, Combined cumulative probability plot of all mIPSCs from all cells recorded under the two buffering conditions; event amplitudes within a neuron were normalized to the mean amplitude in control and then sorted into 25 equal bins, allowing all cells to be pooled. ***B***, Combined cumulative probability plot illustrates the effect of buffering on the rise time. ***C***, Scatter plot of mean charge transfer values at pH 7.4 under the two buffering conditions. ***D***, Effect of pH and buffering on mean charge transfer relative to control. Values at pH 6.8 and 8.0 from $n = 6$ neurons; values at pH 7.4 from $n = 19$ neurons unless otherwise stated. $^{\star}p < 0.05$; $^{\star\star}p < 0.01$; $^{\dagger\dagger}p < 0.0001$.

Synaptic pH is not rigidly maintained by physiological buffering

To determine whether the pH variance observed in 3 mM HEPES (quasi-physiological buffering) is paralleled using physiological buffers, mIPSCs were recorded in 24 mM HCO_3^-/5%CO_2 (control) and were compared with events recorded in 24 mM HCO_3^-/5%CO_2 supplemented with 10 mM HEPES. Figure 3*A* shows raw traces from one neuron under the two conditions. Figure 3*B* shows averaged traces generated from >100 events within one neuron. The cumulative amplitude histogram shows clear reduction caused by HEPES supplementation ($p < 0.0001$, Kolmogorov–Smirnov test) (supplemental Fig. S3*B*, available at www.jneurosci.org as supplemental material). Quantification of all neurons indicates that HEPES supplementation causes a 39% decrease in amplitude (control mean of 65 ± 6.5 pA; $p < 0.0001$, t test; $n = 11$). Normalized averaged traces suggest that increased buffering speeds rise time (supplemental Fig. S3*C*, available at www.jneurosci.org as supplemental material) by 7% (from 0.645 ± 0.032 to 0.601 ± 0.028 ms; $p < 0.05$, t test; $n = 11$) (Fig. 3*C*). A cumulative probability distribution from one cell illustrates the left shift in rise time attributable to increased buffering ($p < 0.0001$, K–S test) (supplemental Fig. S3*D*, available at www.jneurosci.org as supplemental material). Increased buffering also altered the decay kinetics and percentage contribution of fast component to total decay, consistent with alkalinization (supple-

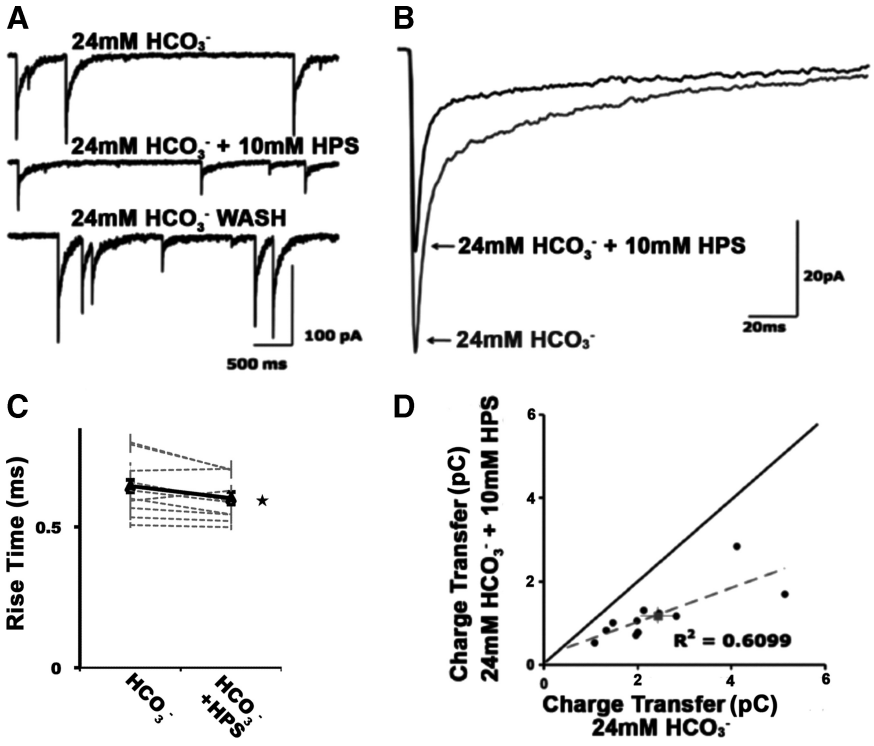

Figure 3. Increased buffering capacity in physiological buffer reduces mIPSC amplitude, rise time, and charge transfer. ***A***, Raw trace from one CGC at −60 mV holding potential shows the effect of increased buffer capacity. ***B***, Averaged traces from one cell (>100 events per condition). ***C***, Effect of increased buffering on rise time. ***D***, As in Figure 2*C*, scatter plot of mean charge transfer values for each neuron under the two buffering conditions. Values from $n = 11$ neurons; $^{\star}p < 0.05$.

mental Fig. S3*E*,*F*, available at www.jneurosci.org as supplemental material).

As predicted by the changes in amplitude and kinetics, increased buffering capacity significantly decreased total charge transfer by ~51% (mean of 2.41 ± 0.36 pC; $p < 0.0001$, *t* test; $n = 11$) (Fig. 3*D*). Event frequency was variable in control (0.41 ± 0.16 Hz) and did not differ significantly with HEPES supplementation (supplemental Fig. S3*A*, available at www.jneurosci.org as supplemental material). Paralleling experiments using solely HEPES buffering, increasing synaptic proton buffering beyond that provided by physiological bicarbonate resulted in significant mIPSC diminishment consistent with alkalinization, further supporting the notion that synaptic pH is labile and ambient pH of the GABAergic synapse is acidified.

HEPES does not inhibit postsynaptic GABAergic transmission

To guard against possible nonspecific effects of HEPES on mIPSCs (Yamamoto and Suzuki, 1987; MacGregor et al., 2001), the following sets of experiments were conducted. First, we acidified the extracellular solution to determine whether "adding protons" could reverse the effect of buffering. At pH 6.8, we found that addition of 24 mM HEPES had no effect on mIPSCs (Fig. 4, compare *A*, *B*). To further divorce the buffering quality of HEPES from potential nonspecific effects, we acidified to pH 6.0 to "overload" (p_{Ka} 7.55) the buffer. As shown in Figure 4*C*, this had no additional effects on mIPSCs (Fig. 4, compare *C*, *A*). Statistical analyses at pH 6.0 show mIPSC amplitudes of 40.4 ± 5.9 in 3 mM and 39.1 ± 4.8 pA in 24 mM HEPES, whereas at pH 6.8 mean amplitude was 43 ± 4.7 in 3 mM and 43 ± 3.8 pA in 24 mM HEPES (pH 6.0, $p = 0.85$; pH 6.8, $p = 0.92$, ANOVA; $n = 6$). Synaptic charge transfer was also unaffected by HEPES at acidic pH (pH 6.0, $p = 0.53$; pH 6.8, $p = 0.72$, ANOVA; $n = 6$). Increased buffering capacity at pH 7.4 sped mIPSC rise time (supplemental Fig. S1*C*, available at www.jneurosci.org as supplemental material) yet had no effect at pH 6.8 ($p = 0.69$, K–S test).

To further attribute the inhibitory effects of HEPES on mIPSCs to its buffering quality, we recorded mIPSCs in the presence of an alternative buffer, PIPES (p_{Ka} 6.80), also at low and high concentrations. At pH 7.4, 24 mM PIPES affected mIPSCs in a similar manner to 24 mM HEPES ($n = 6$) (Fig. 4*D*) (supplemental Fig. S4*A*, available at www.jneurosci.org as supplemental material), i.e., event amplitude decreased by ~26% ($p < 0.05$, ANOVA) (supplemental Fig. S4*C*, available at www.jneurosci.org as supplemental material), rise time sped up ($p < 0.05$, *t* test) (supplemental Fig. S4*D*, available at www.jneurosci.org as supplemental material), the fast component of decay sped up ($p < 0.05$, *t* test) (supplemental Fig. S4*E*, available at www.jneurosci.org as supplemental material), the slow decay component was prolonged ($p < 0.05$, *t* test) (supplemental Fig. S4*F*, available at www.jneurosci.org as supplemental material), and charge transfer was significantly diminished by ~30% ($p < 0.05$, ANOVA) (supplemental Fig. S4*G*, available at www.jneurosci.org as supplemental material). The effects of PIPES could also be reversed by acidification to pH 6.8 ($n = 6$) (Fig. 4*E*) (supplemental Fig. S4*B*, available at www.jneurosci.org as supplemental material). This was further quantified in supplemental Figure S4, *C* and *G* ($n = 6$; ANOVA). We also confirmed that the results obtained at pH 6.0 with HEPES could be replicated with MES (p_{Ka} 6.15) ($n = 5$) (Fig. 4*F*).

Next, we quantified the whole-cell CGC response to exogenous GABA applications at three different pHs under the two proton buffering conditions. At pH 7.4, 24 mM HEPES did not reduce the standardized charge transfer response to 100 μM GABA (103 ± 3% of control; $n = 7$) (Fig. 5*A–C*) and did not affect peak current (I_{peak}) (supplemental Fig. S5*A*, available at www.jneurosci.org as supplemental material), steady-state current (I_{ss}) (supplemental Fig. S6*B*, available at www.jneurosci.org as supplemental material), the percentage of I_{ss} to I_{peak} (supplemental Fig. S5*C*,*D*, available at www.jneurosci.org as supplemental material), the calculated fast and slow time constants of desensitization (supplemental Fig. S5*E*,*F*, available at www.jneurosci.org as supplemental material), or the weighted desensitization constant (supplemental Fig. S5*G*, available at www.jneurosci.org as supplemental material). As has been reported previously (Robello et al., 1994), pH 6.8 significantly enhanced GABA-induced current amplitude and charge transfer values but did not affect desensitization kinetics (Fig. 5) (supplemental Fig. S5, available at www.jneurosci.org as supplemental material). Higher HEPES concentration did not alter the effects of pH 6.8. Response characteristics at pH 6.0 did not differ from control regardless of HEPES concentration (Fig. 5) (supplemental Fig. S5, available at www.jneurosci.org as supplemental material). That increasingly acidic pHs beyond 6.5 do not enhance GABA-

induced responses is consistent with previous reports (Mozrzymas et al., 2003). We also verified the enhancing effect of pH 6.8 to exogenously applied GABA using PIPES and MES buffers and found no specific effects of the buffer on the amplitude or standardized charge transfer (supplemental Fig. S6*A–F*, available at www.jneurosci.org as supplemental material). Together, these results strongly suggest that the HEPES concentrations used in this study do not affect the postsynaptic GABAergic response in a nonspecific manner.

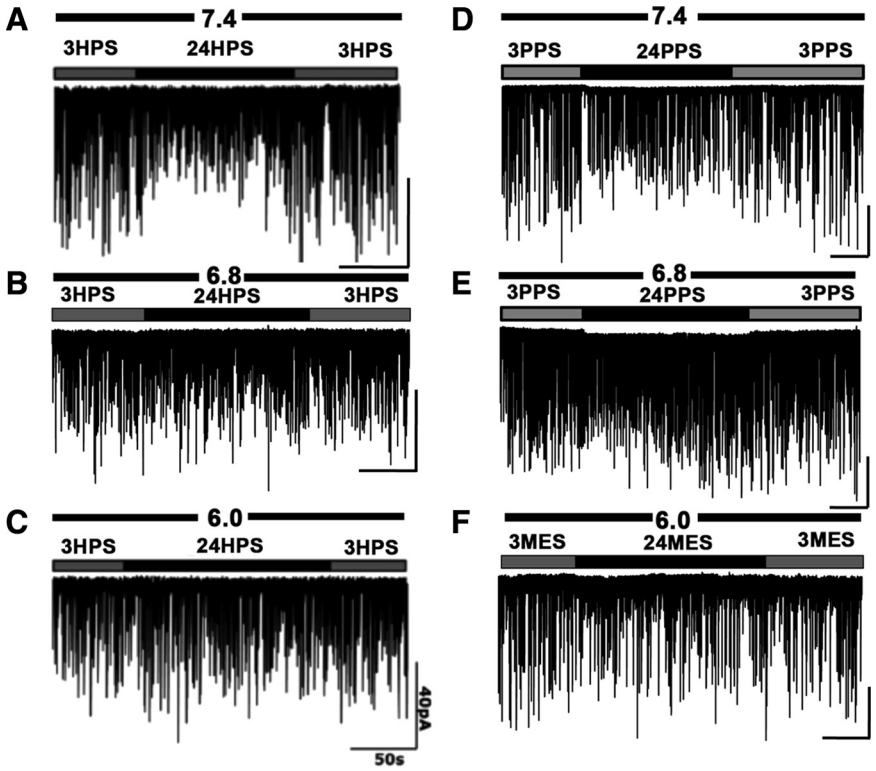

Figure 4. HEPES does not inhibit postsynaptic GABAergic transmission. ***A***, Raw trace from a CGC illustrates the effects of increased HEPES (p_{Ka} 7.55) on mIPSCs at pH 7.4. Bar above trace indicates the application and washout of 24 mM HEPES. ***B***, Raw trace from the same CGC illustrates that addition of HEPES at pH 6.8 does not result in inhibition of mIPSCs. ***C***, Raw trace from a different CGC shows that addition of HEPES at pH 6.0 (overwhelming the buffer with protons) also does not result in mIPSC inhibition. ***D***, Raw trace from a CGC shows that substituting HEPES buffer with PIPES (p_{Ka} 6.80) at pH 7.4 results in inhibition of mIPSCs. ***E***, Raw trace from same CGC as in ***D*** shows that PIPES inhibition of mIPSCs is negated at pH 6.8. ***F***, Raw trace from a different CGC shows that increased buffering with MES (p_{Ka} 6.10) at pH 6.0 has no effect on mIPSCs. Calibration: 40 pA, 50 s. PPS, PIPES.

HEPES does not alter presynaptic GABA release

An alternative explanation for the observed effect of higher HEPES concentrations could be diminished presynaptic release attributable to a nonspecific mechanism. To address this possibility, we recorded mIPSCs under the two buffering conditions in the presence and absence of the benzodiazepine flurazepam. It has been reported that the CGC postsynaptic GABA receptors are saturated by the release of a single vesicle (Wall, 2005). Furthermore, studies have shown that, at saturated neuronal sites, 3 μM flurazepam does not affect mIPSC amplitude (Nusser et al., 1997). If the increased buffering condition were to reduce mIPSC amplitude attributable to diminished presynaptic release (thus changing a saturated site to a subsaturated site), we should expect that flurazepam treatment would preferentially increase mIPSC amplitudes in the condition of increased buffering. Consistent with the notion of saturated CGC sites, we found that flurazepam treatment did not significantly increase mIPSC amplitude in either 3 or 24 mM HEPES buffering ($n = 5$; t test) (supplemental Fig. S7*A*,*B*,*D*, available at www.jneurosci.org as supplemental material). As expected, increased buffering significantly decreased mIPSC amplitude (supplemental Fig. S7*C*, available at www.jneurosci.org as supplemental material). Flurazepam treatment significantly increased the weighted decay constant in both buffering conditions ($p < 0.05$, t test) (supplemental Fig. S7*E–G*, available at www.jneurosci.org as supplemental material). As expected from the increase in decay time, flurazepam treatment significantly increased charge transfer in both buffering conditions, ~38% in 3 mM HEPES and ~30% in 24 mM HEPES ($p < 0.05$, t test) (supplemental Fig. S7*D*, available at www.jneurosci.org as supplemental material). Although the increase in charge transfer was greater in 3 mM HEPES, it was not significantly larger than the increase observed in 24 mM HEPES. Presumably, this increased trend in the lower buffered (and hence more acidic) condition is attributable to the increased efficacy of flurazepam at acidic pH (Wójtowicz et al., 2008). These data support the notion that increased HEPES concentration does not alter presynaptic GABA release.

The Na^+/H^+ exchanger acidifies the GABAergic synapse

Next, we asked the following: what is causing the acidification of the GABAergic synapse? In one set of experiments, we used amiloride at a concentration (20 μM) that is known to induce complete blockade of NHE-1 (K_i of 1.6 μM), half-maximal block of NHE-5 (K_i of 21 μM), and partial block of NHE-3 (K_i of 100 μM) (Szabó et al., 2000). In control quasi-physiological conditions (3 mM HEPES, pH 7.4), addition of amiloride caused mIPSCs to become nearly indistinguishable from the events recorded under higher buffering conditions (10 mM HEPES, pH 7.4) (Fig. 6*A1*). Furthermore, amiloride failed to have any effect in more acidic solutions (pH 6.8) (Fig. 6*A1*). The p_{Ka} of amiloride is 8.4; thus, no change in activity can be attributed to its ionization. Figure 6*A2* shows averaged traces from one cell in control and experimental conditions. Event amplitudes were highly variable (37.12 ± 3.0 pA); thus, amplitude and charge transfer values were calculated relative to control. Amiloride significantly inhibited amplitudes by ~29% ($p < 0.001$, ANOVA; $n = 19$) (supplemental Fig. S8*A1*, available at www.jneurosci.org as supplemental material), and increased buffering (at either 10 or 24 mM HEPES) inhibited amplitudes by ~32% ($p < 0.001$, ANOVA; $n = 17$). Amiloride in the presence of increased buffering inhibited amplitudes by ~33% ($p < 0.001$, ANOVA; $n = 10$). pH 6.8 negated the effects of amiloride ($p = 0.85$; $n = 9$) compared with control. pH 6.8 alone generated mIPSCs that did not differ from those recorded under acidified amiloride ($p = 0.87$; $n = 9$) or control ($p = 0.9$) conditions. At pH 7.4, amiloride sped mIPSC rise time (supplemental Fig. S8*A2*, available at www.jneurosci.org as supplemental material). Cumulative rise time histograms revealed a pronounced left shift attributable to amiloride ($p < 0.0001$, K–S test) (supplemental Fig. S8*A3*, available at www.jneurosci.org as

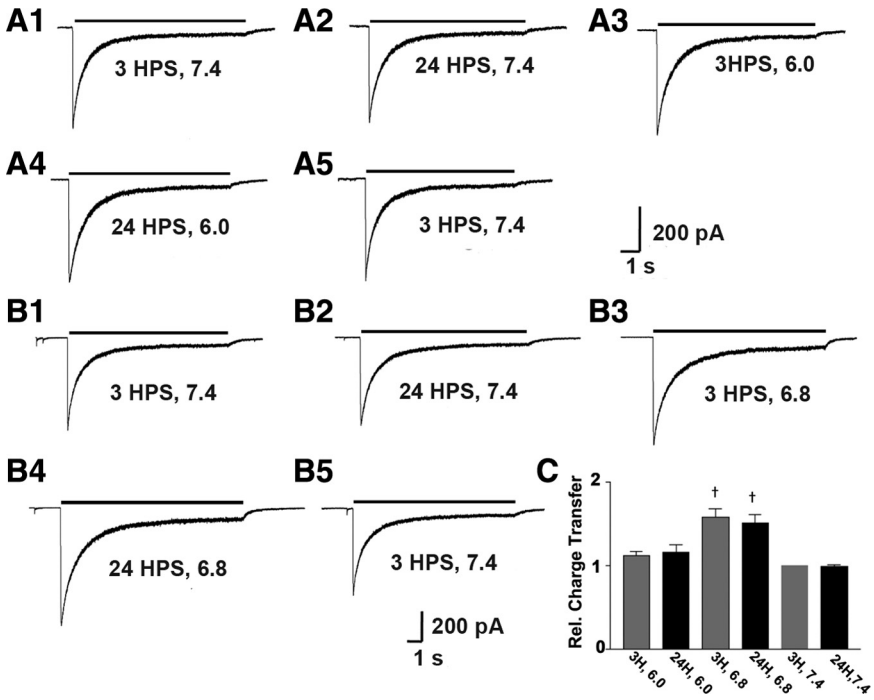

Figure 5. HEPES does not inhibit postsynaptic GABAergic transmission. ***A1–A5***, CGC whole-cell response to rapid application of 100 μM GABA in 3 mM HEPES at pH 7.4 (control), 24 mM HEPES at pH 7.4, 3 mM HEPES at pH 6.0, 24 mM HEPES at pH 6.0, and back to control. ***B1–B5***, CGC whole-cell response to rapid application of 100 μM GABA in 3 mM HEPES at pH 7.4 (control), 24 mM HEPES at pH 7.4, 3 mM HEPES at pH 6.8, 24 mM HEPES at pH 6.8, and back to control. ***C***, Standardized charge transfer evoked by 100 μM GABA in 3 and 24 mM HEPES at the three pH values relative to control. $n = 7$ neurons at pH 7.4, $n = 3$ at pH 6.0, $n = 4$ at pH 6.8. $^{\dagger}p < 0.001$.

supplemental material). Quantitatively, amiloride sped mean rise time by ~7.6% (from 0.691 ± 0.024 to 0.639 ± 0.025 ms; $p < 0.01$, t test; $n = 9$) (supplemental Fig. S8*A4*, available at www.jneurosci.org as supplemental material). Further paralleling the effects of increased buffering, amiloride significantly altered decay kinetics in a manner consistent with alkalinization (supplemental Fig. S8*A5*,*A6*, available at www.jneurosci.org as supplemental material).

As expected, amiloride at pH 7.4 significantly reduced charge transfer from control (1.38 ± 0.25 pC) by ~38% ($p < 0.001$, ANOVA; $n = 19$) (Fig. 6*A3*), comparable with the ~38% reduction by increased buffering ($p < 0.001$, ANOVA; $n = 17$) (Fig. 6*A3*). The combination of increased buffering and amiloride resulted in inhibition equivalent to either condition alone: ~38% ($p < 0.001$, ANOVA; $n = 10$) (Fig. 6*A3*). Events in pH 6.8 plus amiloride did not differ significantly from events in pH 6.8 or control ($p = 0.78$ and $p = 0.88$, respectively, ANOVA; $n = 9$) (Fig. 6*A3*).

In a parallel set of experiments, substituting extracellular sodium with lithium also inhibited NHE. Lithium is known to ride the exchanger at an extremely truncated rate, thus significantly reducing the proton extrusion of NHE (Szabó et al., 2000). Similar to amiloride and increased buffering, lithium replacement in 3 mM HEPES significantly reduced mIPSCs (Fig. 6*B1*). Figure 6*B2* illustrates averaged traces taken from one cell in experimental conditions. Mean control amplitudes were highly variable (65.81 ± 13.74 pA); thus, values were calculated relative to control. Lithium replacement reduced amplitudes by ~29.3% ($p < 0.05$, ANOVA; $n = 3$), whereas increased buffering reduced amplitudes by ~46.3% ($p < 0.01$, ANOVA; $n = 3$), and lithium plus increased buffering reduced this by ~46.8% ($p < 0.05$, ANOVA; $n = 3$) (supplemental Fig. S8*B1*, available at www.jneurosci.org as supplemental material). Lithium substitution sped rise time in a manner similar to strong buffering or alkalinization (supplemental Fig. S8*B2*, available at www.jneurosci.org as supplemental material). Cumulative rise time distributions show a significant left shift in lithium ($p < 0.0001$, K–S test) (supplemental Fig. S8*B3*, available at www.jneurosci.org as supplemental material). Lithium consistently sped average rise time (from 0.690 ± 0.032 to 0.61 ± 0.019 ms) by ~11.6% ($p = 0.07$, t test; $n = 3$) (supplemental Fig. S8*B4*, available at www.jneurosci.org as supplemental material). Lithium replacement altered decay kinetics in a manner consistent with alkalinization (supplemental Fig. S8*B5*,*B6*, available at www.jneurosci.org as supplemental material).

As with amiloride and increased buffering, replacing extracellular sodium with lithium significantly reduced charge transfer by ~51.5% ($p < 0.01$, ANOVA; $n = 3$), similar to the ~54.3% reduction by 24 mM HEPES ($p < 0.05$, ANOVA; $n = 3$) and ~61.8% by lithium plus 24 mM HEPES ($p < 0.01$, ANOVA; $n = 3$) (Fig. 6*B3*).

To illustrate that the NHE inhibitors do not directly antagonize the $GABA_A$ channel at the concentrations used in this study, we recorded whole-cell responses to exogenous application of GABA in the presence of these agents. Coapplication of 20 μM amiloride with 100 μM GABA did not affect response amplitude (99 ± 2% of control; $n = 4$) (supplemental Fig. S9*A*,*C*, available at www.jneurosci.org as supplemental material). Furthermore, amiloride did not affect decay/desensitization kinetics (τ_{fast}, τ_{slow}, or τ_w) of the response (supplemental Fig. S9*D1–D3*, available at www.jneurosci.org as supplemental material). Lithium substitution did not affect the whole-cell response to 100 μM GABA (103 ± 4% of control; $n = 5$) (supplemental Fig. S9*B*,*C*, available at www.jneurosci.org as supplemental material), nor did it affect the response decay/desensitization kinetics (supplemental Fig. S9*E1–E3*, available at www.jneurosci.org as supplemental material). Together, these data suggest that NHE is a critical factor in shaping the pH of, and subsequent transmission at, the GABAergic synapse.

The Na^+/H^+ exchanger acidifies the GABAergic synapse under physiological buffering

To further define the role of NHE, we considered another major neuronal proton extruder, the sodium-dependent anion exchanger (NDAE), which transports sodium and bicarbonate into the cell and extrudes chloride and protons (Kaila and Ransom, 1998). Because NDAE is completely inhibited by removal of extracellular bicarbonate (Kaila, 1994), the HEPES-only experiments might have exaggerated the role of NHE in synaptic acidification.

As in HEPES-only studies, mIPSCs recorded in solutions buffered with 24 mM HCO_3^-/5% CO_2 were suppressed with either 20 μM amiloride or 1 mM LiCl in a manner similar to increased buffering (Fig. 7*A*,*B*). Mean amplitudes were once again highly variable (73.11 ± 9.96 pA); therefore, all values were calculated relative to control. All treatments significantly reduced ampli-

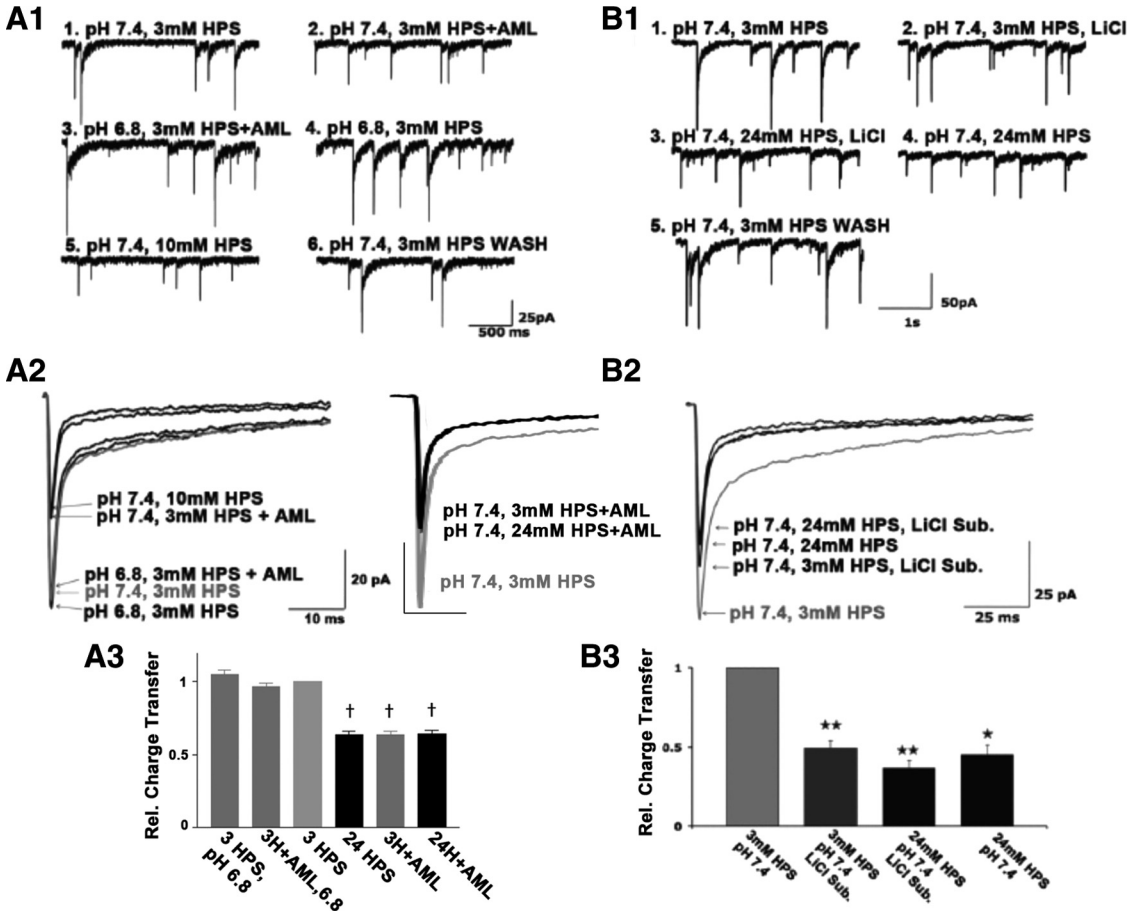

Figure 6. NHE inhibition reduces mIPSC amplitude and charge transfer. ***Series A***, Amiloride at 20 μM (AML) was used to block the NHE. ***A1***, Raw trace sequence from one CGC illustrates the effects of amiloride, protons, amiloride plus protons, and increased buffering on mIPSCs. ***A2***, Left, Averaged traces from one CGC; note that inhibitory effects of amiloride are negated at pH 6.8. ***A2***, Right, Averaged traces from another CGC illustrate the nonadditive effects of amiloride and increased buffering on mIPSCs. Calibration: 40 pA, 10 ms. ***A3***, Effect of experimental amiloride conditions on charge transfer. ***Series B***, NHE block was achieved by substituting extracellular NaCl with LiCl. ***B1***, Raw trace sequence from one CGC illustrates the effects of LiCl replacement, increased buffering capacity, and a combination of the two conditions. ***B2***, Averaged traces from one CGC under the conditions specified. ***B3***, Effects of lithium on charge transfer. $n = 9–19$ neurons in amiloride experiments, $n = 3$ in lithium experiments. $^{\star}p < 0.05$; $^{\star\star}p < 0.01$; $^{\dagger}p < 0.001$.

tude: 1 mM lithium by ~24.4% ($p < 0.001$, ANOVA; $n = 6$), amiloride by ~45.3% ($p < 0.001$, ANOVA; $n = 6$), and addition of 10 mM HEPES by ~45.3% ($p < 0.001$, ANOVA; $n = 5$) (Fig. 7*C*). Amiloride and HEPES both accelerated rise time (supplemental Fig. S10*A*, available at www.jneurosci.org as supplemental material). A cumulative rise time distribution revealed a significant left shift by amiloride ($p < 0.0001$, K–S test) (supplemental Fig. S10*B*, available at www.jneurosci.org as supplemental material) but not lithium ($p = 0.58$, K–S test) (supplemental Fig. S10*B*, available at www.jneurosci.org as supplemental material). A combined cumulative rise time histogram showed a significant effect of amiloride ($p < 0.0001$, Mann–Whitney *U* test; $n = 633$ events in control, 533 events in amiloride) (supplemental Fig. S10*C*, available at www.jneurosci.org as supplemental material). Changes in decay kinetics attributable to NHE inhibition were also consistent with alkalinization (supplemental Fig. S10*D–F*, available at www.jneurosci.org as supplemental material). Control mIPSC frequency (0.48 ± 0.11 Hz) was not significantly altered by drugs or buffering, although trends to increase in lithium and amiloride were observed, consistent with previous work (Jang et al., 2006) (supplemental Fig. S10*G*, available at www.jneurosci.org as supplemental material).

As expected, both forms of NHE inhibition significantly decreased charge transfer from control (2.72 ± 0.51 pC). Lithium at 1 mM reduced charge transfer by ~28.7% ($p < 0.001$, ANOVA; $n = 6$), amiloride reduced this by ~63.5% ($p < 0.0001$, ANOVA; $n = 6$), and increased buffering reduced charge transfer by ~61.1% ($p < 0.0001$, ANOVA; $n = 6$) (Fig. 7*D*). Our data therefore provide little support for NDAE in acidification of synaptic nano-environment in addition to NHE.

Discussion

The major finding of this report is that the physiological proton buffering capacity at the synaptic cleft allows for unique endogenous modulation of GABAergic mIPSC amplitudes and kinetics consistent with acidification. We demonstrate that generally used experimental solutions buffered by 10 mM or more HEPES cause changes to mIPSCs that mimic alkalinization, thus masking the endogenous acidification of the synapse (Figs. 1–3). We have identified NHE as a critical factor in this synaptic acidification (Figs. 6, 7), a finding consistent with both its localization to cerebellar inhibitory neurons (Ma and Haddad, 1997; Douglas et al., 2001) and its high activity at GABAergic presynaptic terminals (Jang et al., 2006). We suggest that, under physiological conditions, protons extruded by the NHE overwhelm the buffering capacity of the confined synaptic space and the resultant acidification alters mIPSC amplitude and kinetics, thereby effectively doubling the charge transferred by each event. We base this hy-

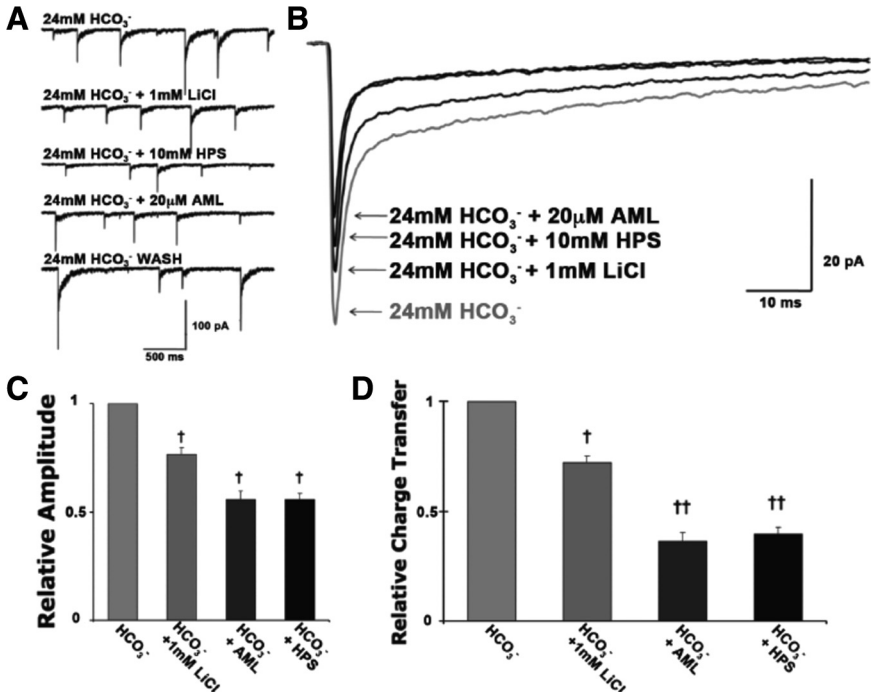

Figure 7. NHE inhibition in bicarbonate buffering reduces mIPSC amplitude and charge transfer. ***A***, Raw traces from one CGC illustrate the effects of buffering and NHE inhibition under physiological buffering. ***B***, Averaged mIPSCs derived from >100 events per condition. ***C***, Quantified mean amplitudes relative to control. ***D***, Effects of increased buffering and NHE inhibition on charge transfer relative to control. $n = 6$ neurons. $^{\dagger}p < 0.001$; $^{\dagger\dagger}p < 0.0001$. AML, Amiloride.

pothesis on the following observations. First, adding protons back into the system (decreasing pH) negated the effects of both increased buffering and NHE inhibition (Figs. 4, 6) (supplemental Fig. S4, available at www.jneurosci.org as supplemental material). Second, flurazepam experiments indicate that increased HEPES does not diminish quantal release of GABA (supplemental Fig. S7, available at www.jneurosci.org as supplemental material). Third, mIPSC diminishment attributable to NHE inhibition occurred without changes to HEPES buffering (Figs. 6, 7). Fourth, all three agents used in our study to counteract synaptic acidification (10–24 mM HEPES, amiloride, and lithium) decreased mIPSC amplitude and sped rise time. The only conditions known to speed $GABA_A$ current rise times are increased agonist concentration (Jones et al., 2001) and alkalinization (Mozrzymas et al., 2003); of these two, only alkalinization results in amplitude decrease. Finally, neither the HEPES concentration nor the NHE inhibitors that altered mIPSCs had effect on whole-cell responses to exogenously applied GABA (Fig. 5) (supplemental Figs. S6, S9, available at www.jneurosci.org as supplemental material). This last point must be qualified with the notion that the channels that comprise the whole-cell response are a heterogeneous population of receptors known to be of both synaptic and extrasynaptic varieties (Nusser et al., 1998).

We believe this model is appealing when paralleled to studies reporting alkalinization at excitatory synapses (Makani and Chesler, 2007) because, just as alkalinization will maintain the fidelity of NMDA transmission, acidification will ensure the best GABAergic "bang for the buck."

Physiological relevance

This work provides evidence that GABAergic synapses onto CGCs are acidified by proton extrusion via NHE; this in turn leads to enhancement of the postsynaptic response to a single vesicle. This signaling role of NHEs, first identified in muscle contraction of *C. elegans* (Beg et al., 2008), appears to be preserved in the mammalian CNS. In the CNS, neuronal NHE expression for most isoforms is greatest in inhibitory neurons (Douglas et al., 2001; Jang et al., 2006) and increases with age (Ma and Haddad, 1997; Lin et al., 2003). The potential contribution of NHEs to conditions of pathological extracellular acidification, such as hypoxia, ischemia, and hypoglycemia (Katsura and Siesjo, 1998), must now be reconsidered in light of these findings. This study opens new mechanistic insights into disorders arising from NHE dysfunction, including growth retardation, ataxia, and seizure (Cox et al., 1997; Bell et al., 1999). It is intriguing to speculate, for instance, that certain seizures may arise from compromised NHE function, resulting in reduced GABAergic drive, thus opening the door to runaway excitation. The converse, NHE overexpression, could lead to enhanced inhibition. Indeed, increased NHE expression has been correlated with loss of respiratory drive in rabbits (Kiwull-Schöne et al., 2007) and clinically with sudden infant death syndrome (Wiemann et al., 2008).

Our study also suggests that therapeutic concentrations of lithium (1 mM) (Watanabe et al., 1973) may significantly inhibit NHE-mediated amplification of GABAergic neurotransmission. This finding, although surely not the only mechanism of lithium therapy, might set the stage for additional investigations into the NHE–GABAergic role on mood-altering disorders (Nemergut, 2005), lithium toxicity-induced seizure (el-Mallakh and Lee, 1987), and lithium–pilocarpine-induced animal seizure models (Kaminski et al., 2007).

Experimental model

In this study, cultured CGC neurons were used rather than brain slices. For the purpose of these experiments, this paradigm offers several critical advantages. First, as opposed to large hippocampal pyramidal cells, CGCs are small (5–8 μm diameter, 4–7 pF capacitance), with four to five short (<30 μm), thin (<0.2 μm) dendrites (Llinas and Sotelo, 1992), allowing reliable voltage control and thus high-fidelity synaptic recordings (Losi et al., 2003). Second, neuronal cultures, as opposed to brain slices, are not subject to potential regional pH heterogeneity (MacGregor et al., 2001) or aberrant pH buffering caused by intracellular carbonic anhydrase release from sliced cells (Voipio et al., 1995). Furthermore, cultures allow for rapid and reliable superfusion/exchange of test solutions and thus allow for valid assessment of solution washout and return to baseline response. That said, the true physiological relevance of these findings would not fully be appreciated until these experiments can be performed in more physiological preparations such as the slice. Certain factors critical to pH regulation, namely glial ensheathment of the synapse (potentially further confining proton diffusion) and the intrinsic geometry of the synapse could result in the amplification of the acidification seen at the cleft.

Although we believe that we have put forth a compelling role for the NHE as a prominent source of synaptic acidification, it should be noted that the synaptic vesicle itself is known to be

highly acidic (Miesenböck et al., 1998). In our study, we have examined only the modulation of single vesicle exocytosis. Under conditions of increased action-potential-driven release, it may be very likely that the buffering of the synapse is further challenged by vesicular proton release, as is the case at the retinal ribbon synapse (DeVries, 2001).

Concluding remarks

Our data illustrates the physiological relevance of previous work that meticulously cataloged the effects of acidification on ion channels in general and GABA receptors in particular. Additionally, we show for the first time that the physiological buffering capacity of the synaptic cleft is sufficiently flexible as to allow endogenous acidification to occur, resulting in enhanced inhibitory signaling at these GABAergic synapses of the mammalian brain.

References

Beg AA, Ernstrom GG, Nix P, Davis MW, Jorgensen EM (2008) Protons act as a transmitter for muscle contraction in *C. elegans*. Cell 132:149–160.

Bell SM, Schreiner CM, Schultheis PJ, Miller ML, Evans RL, Vorhees CV, Shull GE, Scott WJ (1999) Targeted disruption of the murine Nhe1 locus induces ataxia, growth retardation, and seizures. Am J Physiol 276:C788–C795.

Chen L, Chetkovich DM, Petralia RS, Sweeney NT, Kawasaki Y, Wenthold RJ, Bredt DS, Nicoll RA (2000) Stargazin regulates synaptic targeting of AMPA receptors by two distinct mechanisms. Nature 408:936–943.

Chesler M, Kaila K (1992) Modulation of pH by neuronal activity. Trends Neurosci 15:396–402.

Cox GA, Lutz CM, Yang CL, Biemesderfer D, Bronson RT, Fu A, Aronson PS, Noebels JL, Frankel WN (1997) Sodium/hydrogen exchanger gene defect in slow-wave epilepsy mutant mice. Cell 91:139–148.

Davies NW, Lux HD, Morad M (1988) Site and mechanism of activation of proton-induced sodium current in chick dorsal root ganglion neurones. J Physiol 400:159–187.

DeVries SH (2001) Exocytosed protons feedback to suppress the Ca^{2+} current in mammalian cone photoreceptors. Neuron 32:1107–1117.

Douglas RM, Schmitt BM, Xia Y, Bevensee MO, Biemesderfer D, Boron WF, Haddad GG (2001) Sodium-hydrogen exchangers and sodium-bicarbonate co-transporters: ontogeny of protein expression in the rat brain. Neuroscience 102:217–228.

el-Mallakh RS, Lee RH (1987) Seizures and transient cognitive deterioration as sequelae of acute lithium intoxication. Vet Hum Toxicol 29:143–145.

Fedirko N, Svichar N, Chesler M (2006) Fabrication and use of high-speed, concentric H^+- and Ca^{2+}-selective microelectrodes suitable for in vitro extracellular recording. J Neurophysiol 96:919–924.

Iijima T, Ciani S, Hagiwara S (1986) Effects of the external pH on Ca channels: experimental studies and theoretical considerations using a two-site, two-ion model. Proc Natl Acad Sci U S A 83:654–658.

Jang IS, Brodwick MS, Wang ZM, Jeong HJ, Choi BJ, Akaike N (2006) The Na^+/H^+ exchanger is a major pH regulator in GABAergic presynaptic nerve terminals synapsing onto rat CA3 pyramidal neurons. J Neurochem 99:1224–1236.

Jones MV, Jonas P, Sahara Y, Westbrook GL (2001) Microscopic kinetics and energetics distinguish $GABA_A$ receptor agonists from antagonists. Biophys J 81:2660–2670.

Kaila K (1994) Ionic basis of GABAA receptor channel function in the nervous system. Prog Neurobiol 42:489–537.

Kaila K, Ransom BR (1998) pH and brain function. New York: Wiley.

Kaminski RM, Blaszczak P, Dekundy A, Parada-Turska J, Calderazzo L, Cavalheiro EA, Turski WA (2007) Lithium-methomyl induced seizures in rats: a new model of status epilepticus? Toxicol Appl Pharmacol 219:122–127.

Katsura K, Siesjo BK (1998) Acid-base metabolism in ischemia. In: pH and brain function (Kaila K, Ransom BR, eds), pp 563–582. New York: Wiley.

Kiwull-Schöne H, Kiwull P, Frede S, Wiemann M (2007) Role of brainstem sodium/proton exchanger 3 for breathing control during chronic acid base imbalance. Am J Respir Crit Care Med 176:513–519.

Kraig RP, Ferreira-Filho CR, Nicholson C (1983) Alkaline and acid transients in cerebellar microenvironment. J Neurophysiol 49:831–850.

Krishtal OA, Pidoplichko VI (1981) Receptor for protons in the membrane of sensory neurons. Brain Res 214:150–154.

Lin WM, Chen XH, Xu R, Liu X, Xu P (2003) Tissue-specific expression of Na^+-H^+ exchanger isoforms at two developmental stages of human fetus (in Chinese). Sheng Li Xue Bao 55:79–82.

Llinas RR, Sotelo (1992) The cerebellum revisited. New York: Springer.

Losi G, Prybylowski K, Fu Z, Luo J, Wenthold RJ, Vicini S (2003) PSD-95 regulates NMDA receptors in developing cerebellar granule neurons of the rat. J Physiol 548:21–29.

Ma E, Haddad GG (1997) Expression and localization of Na^+/H^+ exchangers in rat central nervous system. Neuroscience 79:591–603.

MacGregor DG, Chesler M, Rice ME (2001) HEPES prevents edema in rat brain slices. Neurosci Lett 303:141–144.

Makani S, Chesler M (2007) Endogenous alkaline transients boost postsynaptic NMDA receptor responses in hippocampal CA1 pyramidal neurons. J Neurosci 27:7438–7446.

Mathews GC, Diamond JS (2003) Neuronal glutamate uptake contributes to GABA synthesis and inhibitory synaptic strength. J Neurosci 23:2040–2048.

Miesenböck G, De Angelis DA, Rothman JE (1998) Visualizing secretion and synaptic transmission with pH-sensitive green fluorescent proteins. Nature 394:192–195.

Mozrzymas JW, Zarnowska ED, Pytel M, Mercik K (2003) Modulation of $GABA_A$ receptors by hydrogen ions reveals synaptic GABA transient and a crucial role of the desensitization process. J Neurosci [Erratum (2003) 23:following 9003; Zarmowska ED (corrected to Zarnowska ED)] 23:7981–7992.

Nemergut EC (2005) Perioperative drug manual, Ed 2. Philadelphia: Elsevier-Saunders.

Nusser Z, Cull-Candy S, Farrant M (1997) Differences in synaptic $GABA_A$ receptor number underlie variation in GABA mini amplitude. Neuron 19:697–709.

Nusser Z, Sieghart W, Somogyi P (1998) Segregation of different GABAA receptors to synaptic and extrasynaptic membranes of cerebellar granule cells. J Neurosci 18:1693–1703.

Palmer MJ, Hull C, Vigh J, von Gersdorff H (2003) Synaptic cleft acidification and modulation of short-term depression by exocytosed protons in retinal bipolar cells. J Neurosci 23:11332–11341.

Robello M, Baldelli P, Cupello A (1994) Modulation by extracellular pH of the activity of GABAA receptors on rat cerebellum granule cells. Neuroscience 61:833–837.

Shuba YM, Dietrich CJ, Oermann E, Cleemann L, Morad M (2008) Local extracellular acidification caused by Ca^{2+}-dependent exocytosis in PC12 cells. Cell Calcium 44:220–229.

Szabó EZ, Numata M, Shull GE, Orlowski J (2000) Kinetic and pharmacological properties of human brain Na^+/H^+ exchanger isoform 5 stably expressed in Chinese hamster ovary cells. J Biol Chem 275:6302–6307.

Tang CM, Dichter M, Morad M (1990) Modulation of the *N*-methyl-D-aspartate channel by extracellular H^+. Proc Natl Acad Sci U S A 87:6445–6449.

Traynelis SF, Cull-Candy SG (1990) Proton inhibition of *N*-methyl-D-aspartate receptors in cerebellar neurons. Nature 345:347–350.

Voipio J, Paalasmaa P, Taira T, Kaila K (1995) Pharmacological characterization of extracellular pH transients evoked by selective synaptic and exogenous activation of AMPA, NMDA, and GABAA receptors in the rat hippocampal slice. J Neurophysiol 74:633–642.

Waldmann R, Lazdunski M (1998) H^+-gated cation channels: neuronal acid sensors in the NaC/DEG family of ion channels. Curr Opin Neurobiol 8:418–424.

Wall MJ (2005) Alterations in GABAA receptor occupancy occur during the postnatal development of rat Purkinje cell but not granule cell synapses. Neuropharmacology 49:596–609.

Watanabe S, Taguchi K, Ebara T, Iguchi K, Otsuki S (1973) Lithium concentration in cerebrospinal fluid of affective psychotic patients treated with lithium carbonate and its clinical response. Folia Psychiatr Neurol Jpn 27:299–303.

Wiemann M, Frede S, Tschentscher F, Kiwull-Schöne H, Kiwull P, Bingmann D, Brinkmann B, Bajanowski T (2008) NHE3 in the human brainstem: implication for the pathogenesis of the sudden infant death syndrome (SIDS)? Adv Exp Med Biol 605:508–513.

Wójtowicz T, Wyrembek P, Lebida K, Piast M, Mozrzymas JW (2008) Flurazepam effect on GABAergic currents depends on extracellular pH. Br J Pharmacol 154:234–245.

Yamamoto D, Suzuki N (1987) Blockage of chloride channels by HEPES buffer. Proc R Soc Lond B Biol Sci 230:93–100.